

Rotating non-Kerr black hole and energy extraction

Changqing Liu^{1,2}, Songbai Chen¹, and Jiliang Jing^{1*}

*1) Department of Physics, and Key Laboratory of Low Dimensional Quantum Structures
and Quantum Control of Ministry of Education, Hunan Normal University,*

Changsha, Hunan 410081, P. R. China and

*2) Department of Physics and Information Engineering,
Hunan Institute of Humanities Science and Technology,
Loudi, Hunan 417000, P. R. China*

Abstract

The properties of the ergosphere and energy extraction by Penrose process in a rotating non-Kerr black hole are investigated. It is shown that the ergosphere is sensitive to the deformation parameter ϵ and the shape of the ergosphere becomes thick with increase of the parameter ϵ . It is of interest to note that, comparing with the Kerr black hole, the deformation parameter ϵ can enhance the maximum efficiency of the energy extraction process greatly. Especially, for the case of $a > M$, the non-Kerr metric describes a superspinning compact object and the maximum efficiency can exceed 60%, while it is only 20.7% for the extremal Kerr black hole.

PACS numbers: 04.70.Dy, 95.30.Sf, 97.60.Lf

Keywords: Energy Extraction, Rotating non-Kerr black hole, Penrose process

* Corresponding author, Email: jljing@hunnu.edu.cn

I. INTRODUCTION

In 4-dimensional general relativity, no-hair theorem [1] guarantees that a neutral rotating astrophysical black hole is uniquely described by the Kerr metric which only possesses two parameters, the mass M and the rotational parameter a . For the Kerr black hole, the fundamental limit is the bound $a \leq M$, and the central singularity is always behind the event horizon due to the weak cosmic censorship conjecture [2]. However, the hypothesis that the astrophysical black-hole candidates are described by the Kerr metrics still lacks the direct evidence, and the general relativity has been tested only for weak gravitational fields [3]. In the regime of strong gravity, the general relativity could be broken down and astrophysical black holes might not be the Kerr black holes as predicted by the no-hair theorem [4–6]. Several parametric deviations from the Kerr metric have been suggested to study observational signatures in both the electromagnetic [7] and gravitational-wave [8] spectral that differ from the expected Kerr signals.

Recently, Johannsen and Psaltis proposed a deformed Kerr-like metric [5] suitable for the strong field of the no-hair theorem, which describes a rotating black hole (we named it the non-Kerr black hole) in an alternative theory of gravity beyond Einstein’s general relativity. The non-Kerr black hole possesses the following novel features: there is no restriction on the value of the rotational parameter a due to the existence of the deformation parameter ϵ . Interestingly, for a positive parameter ϵ , the non-Kerr black hole becomes more prolate than the Kerr black hole and there are two disconnected horizons for high spin parameters, but there is no horizon when $a > M$. Therefore, for a negative parameter ϵ , the non-Kerr black hole is more oblate than the Kerr black hole, and the horizon always exists for an arbitrary a and the topology of the horizon becomes toroidal [6, 9]. The non-Kerr metric is an ideal spacetime to carry out strong-field tests of the no-hair theorem. Therefore, a lot of effort has been dedicated to the study of the rotating non-Kerr black hole recently [4–6, 9–12]. In Ref. [13], we studied the properties of the thin accretion disk in the rotating non-Kerr spacetime and found that the presence of the deformation parameter ϵ changes the inner border of the disk, energy flux, conversion efficiency, radiation temperature, spectral luminosity and spectral cut-off frequency of the thin accretion disk. Moreover, for the rapidly rotating black

hole, the effect of the deformation parameter ϵ on the physical quantities of the thin disk becomes more distinct for the prograde particles and more tiny for the retrograde ones. These significant features in the mass accretion process may provide a possibility to test gravity in the regime of the strong field in the astronomical observations.

The power energy for a active galactic nuclei, X-ray binaries and quasars has always been concerned in the high energy astrophysics. Several mechanisms (i.e. the accretion disk model [14, 15] and Blandford-Znajek mechanism [16]) have been proposed to interpret how to extract energy from a black hole and the formation of the power jet. Furthermore, the Penrose process [2, 17, 19] also provides an important method to extract energy from a black hole. The Penrose process was also extended to the five-dimensional supergravity rotating black hole [20], higher dimensional black holes and black rings [21], and Hořava-Lifshitz Gravity [22]. In this paper, we will investigate in detail the ergosphere of the non-Kerr black hole and how the deformation parameter ϵ of the non-Kerr black hole affects the negative energy state and the efficiency of the energy extraction.

The paper is organized as follows: in Sec. II, we review briefly the metric of the rotating non-Kerr black hole proposed by Johannsen and Psaltis [5] to test gravity in the regime of the strong field and then analyze the ergosphere structure. In Sec. III, we investigate the efficiency of the energy extraction by using the Penrose process. Sec. IV is devoted to a brief summary.

II. ROTATING NON-KERR BLACK HOLE SPACETIME

To test gravity in the regime of the strong field, Johannsen and Psaltis [5], starting from a deformed Schwarzschild solution and applying the Newman-Janis transformation, constructed a deformed Kerr-like metric which describes a stationary, axisymmetric, and asymptotically flat vacuum spacetime. In the standard Boyer-Lindquist coordinates, the metric can be expressed as [5]

$$ds^2 = g_{tt}dt^2 + g_{rr}dr^2 + g_{\theta\theta}d\theta^2 + g_{\phi\phi}d\phi^2 + 2g_{t\phi}dtd\phi, \quad (2.1)$$

with

$$\begin{aligned}
g_{tt} &= -\left(1 - \frac{2Mr}{\rho^2}\right)(1+h), & g_{t\phi} &= -\frac{2aMr \sin^2 \theta}{\rho^2}(1+h), \\
g_{rr} &= \frac{\rho^2(1+h)}{\Delta + a^2 h \sin^2 \theta}, & g_{\theta\theta} &= \rho^2, \\
g_{\phi\phi} &= \sin^2 \theta \left[\rho^2 + \frac{a^2(\rho^2 + 2Mr) \sin^2 \theta}{\rho^2}(1+h) \right],
\end{aligned} \tag{2.2}$$

where

$$\rho^2 = r^2 + a^2 \cos^2 \theta, \quad \Delta = r^2 - 2Mr + a^2, \quad h = \frac{\epsilon M^3 r}{\rho^4}. \tag{2.3}$$

The constant ϵ is the deformation parameter. The quantity $\epsilon > 0$ or $\epsilon < 0$ corresponds to the cases in which the compact object is more prolate or oblate than the Kerr black hole, respectively. As $\epsilon = 0$, the black hole is reduced to the usual Kerr black hole in general relativity. The horizons of the black hole are described by the roots of the following equation [5]

$$\Delta + a^2 h \sin^2 \theta = 0. \tag{2.4}$$

Clearly, the radii of the horizons depends on θ , which are different from that in the usual Kerr case. For the case of $\epsilon > 0$, there exist two disconnected horizons for high spin parameters, but there is no horizon when $a > M$. However, for $\epsilon < 0$ the horizons never disappear for an arbitrary a and the shape of the horizons becomes toroidal [6, 9].

The infinite redshift surface of a black hole is defined by the roots of $g_{tt} = 0$. For the non-Kerr black hole we note that $g_{tt} = 0$ gives

$$1 + h = 0, \quad \text{or} \quad 1 - \frac{2Mr}{\rho^2} = 0. \tag{2.5}$$

Obviously, for the case of $\epsilon \geq 0$, the outer infinite redshift surface is determined by $M + \sqrt{M^2 - a^2 \cos^2 \theta}$. For $\epsilon < 0$, it seems that both of the positive root of $1 + h = 0$ and $1 - \frac{2Mr}{\rho^2} = 0$ are the infinite redshift surfaces of the non-Kerr black hole. However, the

determinant of the metric $\sqrt{-g} = (1+h)\rho^2 \sin\theta^2$ vanishes if $1+h=0$ which shows that the surface defined by $1+h=0$ is an intrinsic singularity. The singularity is indicated by infinite curvature and cannot be eliminated by coordinate transformation, and it's Kretschmann scalar $K = R^{\alpha\beta\gamma\delta}R_{\alpha\beta\gamma\delta}$ and $\sqrt{-g}$ becomes zero or infinity. In Fig. 1, we depict the positive root of the equations $1+h=0$, $1-\frac{2Mr}{\rho^2}=0$, and $\Delta+a^2h\sin^2\theta=0$ with different deformation parameter ϵ . The figure also shows that the surface defined by $1+h=0$ is the intrinsic singularity, because if we choose the surface defined by $1+h=0$ as the outer infinite redshift surface, we find that the metric of the non-Kerr black hole does not satisfy $g_{tt} > 0$, $g_{t\phi} < 0$ and $g_{rr} > 0$ in the ergosphere and the causality of the spacetime is violated. Thus the surface defined by $1+h=0$ cannot be the infinite redshift surface. In Fig. 1, there is an intersection point of the three surfaces and the value of the abscissa for the intersection point ϵ_{ip} is $-4(M + \sqrt{M^2 - a^2\cos^2\theta})$. There also exists a turning point ϵ_{tp} for the event horizon surface. The value of the abscissa for the turning point is located at the position $\frac{\partial\epsilon}{\partial r} = 0$, thus we get

$$10r^4 - 16Mr^3 + a^2(7 + \cos(2\theta))r^2 - a^4(1 + \cos(2\theta)) = 0. \quad (2.6)$$

The maximum positive root of Eq. (2.6) is

$$\begin{aligned} r_{tp} &= \frac{1}{2} \left(\frac{-A}{2} + \sqrt{Z_1} + \sqrt{\frac{3A^3}{4} - 2B - Z_1 + \frac{-A^3 + 4AB}{4\sqrt{Z_1}}} \right) \\ Z_1 &= \frac{A^2}{4} - \frac{2B}{3} + \frac{2^{1/3}(B^2 + 12C)}{3Z_2^{1/3}} + \frac{Z_2^{1/3}}{3 \cdot 2^{1/3}} \\ Z_2 &= 2B^3 + 27A^2C - 72BC + \sqrt{-(4B^2 + 12C) + (2B^3 + 27A^2C - 72BC)^2} \\ A &= -\frac{8M}{5}, \quad B = \frac{a^2(7 + \cos(2\theta))}{10}, \quad C = -\frac{a^4(1 + \cos(2\theta))}{10}. \end{aligned} \quad (2.7)$$

Using the Eqs. (2.6) and (2.7), we get the value of the abscissa for the turning point of the curve described by $\Delta + a^2h\sin^2\theta = 0$, which is

$$\epsilon_{tp} = \left. \frac{-\Delta\rho^4}{M^3a^2r\sin^2\theta} \right|_{r=r_{tp}}. \quad (2.8)$$

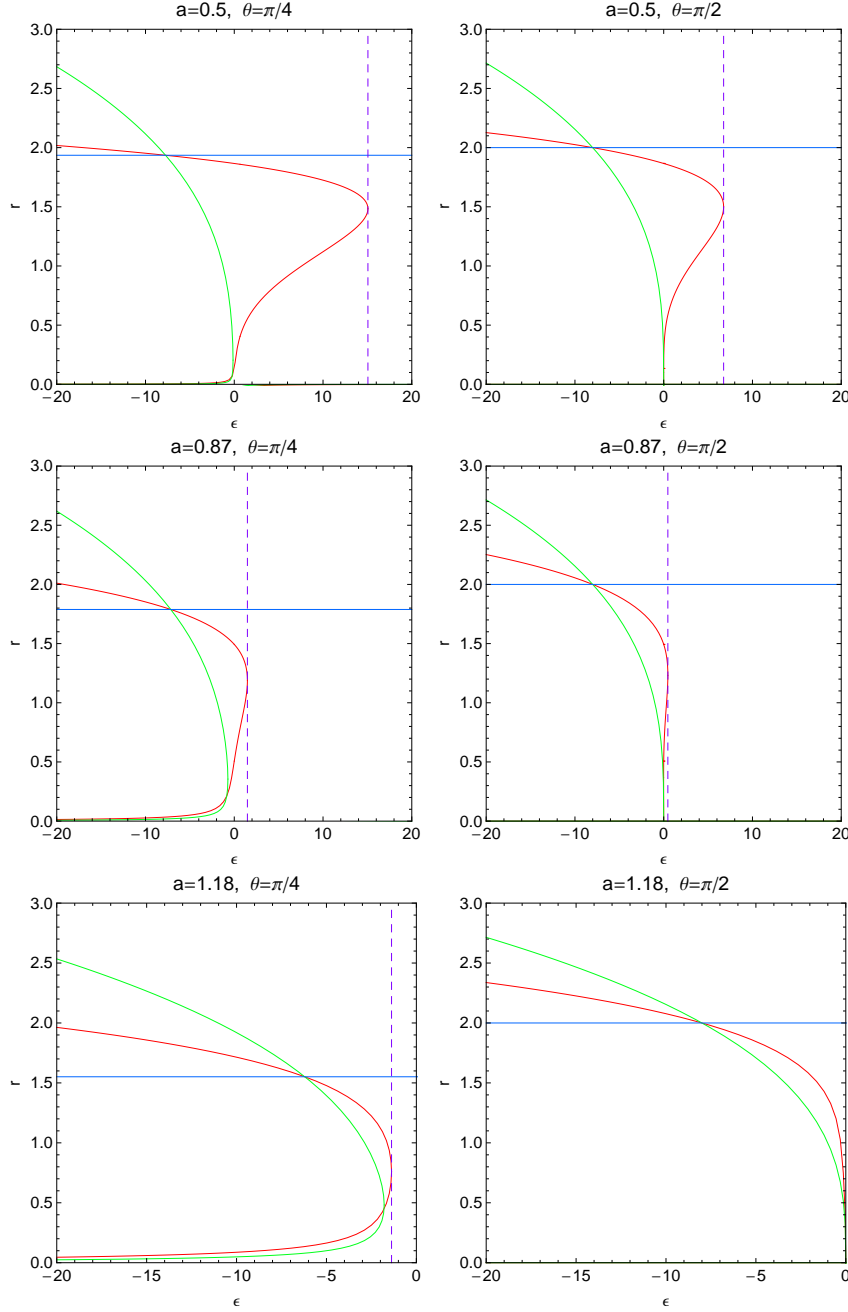


FIG. 1: The variation of the event horizon radius and the outer infinite redshift surface radius with the deformation parameter ϵ of the rotating non-Kerr black hole. The green, blue, and red lines correspond to the surfaces defined by $1 + h = 0$, $1 - \frac{2Mr}{\rho^2} = 0$, and $\Delta + a^2 h \sin^2 \theta = 0$, respectively. The dashed line is the location of turning point of the surface defined by $\Delta + a^2 h \sin^2 \theta = 0$. Here, we take $M = 1$.

The ergosphere is the region bounded by the event horizon r_H and the outer stationary limit surface r_∞ . A novel feature of the ergosphere of a black hole is that the timelike Killing vector becomes spacelike crossing the infinite redshift surface. An observer moving along the timelike geodesics cannot remain static but stationary in the ergosphere due to the “frame-dragging effect” [3]. According to the properties of the ergosphere, the deformation parameter ϵ should satisfy following relation

$$-4(M + \sqrt{M^2 - a^2 \cos^2 \theta}) \leq \epsilon \leq \frac{\Delta \rho^4}{M^3 a^2 r \sin^2 \theta} \Big|_{r=r_{tp}}. \quad (2.9)$$

In this range of ϵ , the non-Kerr black hole has a event horizon given by largest root of $\Delta + a^2 h \sin^2 \theta = 0$, and a outer infinite redshift surface described by

$$r_\infty^+ = M + \sqrt{M^2 - a^2 \cos^2 \theta}. \quad (2.10)$$

When $\epsilon \geq \epsilon_{tp}$ or $\epsilon < \epsilon_{ip}$ there is no the event horizon and the singularity becomes naked.

How the deformation parameter ϵ affects the shape of the ergosphere is described by Fig. 2 which shows that the ergosphere is sensitive to the deformation parameter ϵ . For $a < M$ (such as $a = 0.87$), the non-Kerr black hole becomes more prolate than the Kerr black hole, and the ergosphere in the equatorial plane becomes thick as the parameter ϵ increases. It should be pointed out that, when ϵ exceed 4.4676, the horizons become disconnected. For the case of $a = M$, there exist the inner and outer horizons which coincide at the north and south poles, and the thickness of the ergosphere decreases when the deformation parameter ϵ takes a bigger negative value. For $a > M$, ϵ can only take a negative value, and both the horizon and infinite redshift surface are not closed. A hole appears around the north and south poles in the range $\theta_{hole} \leq \arccos(a/M)$. Thus a distant observer may see the central region of this compact object along the north or south pole. It is also interesting to note that the overspin compact object becomes more and more thin and looks like a disk [6] as the deformation parameter ϵ increases.

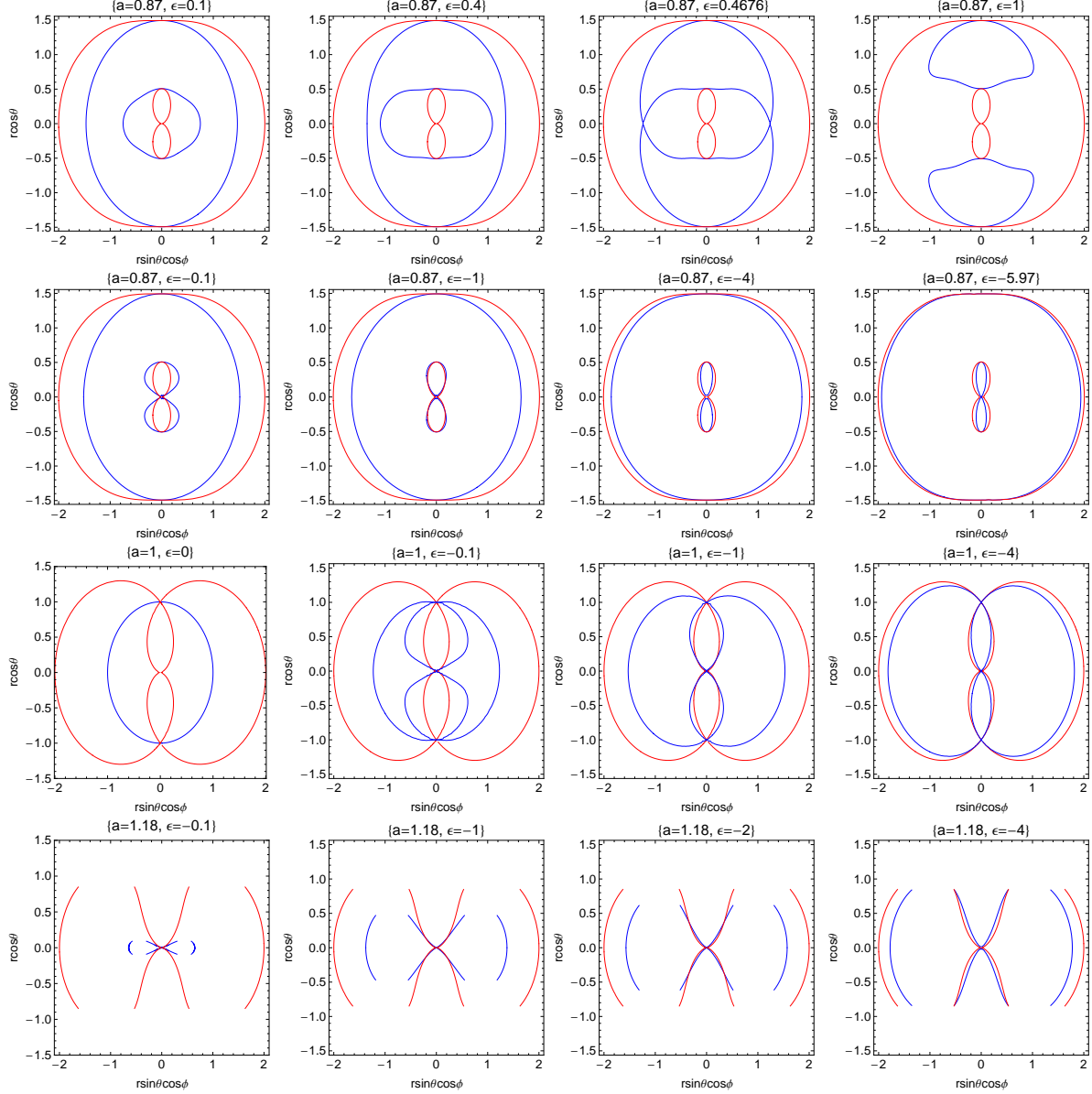


FIG. 2: The variation of the shape of the xz -plane of the ergosphere with the deformation parameter ϵ of the rotating non-Kerr black hole. The red and the blue lines correspond to the infinite redshift surfaces and the horizons, respectively. Here, we take $M = 1$.

III. ENERGY EXTRACTION OF THE BLACK HOLE BY PENROSE PROCESS

In this section, we will discuss the Penrose process [2, 17, 19, 21], by which we can extract a rotational energy from the non-Kerr black hole. We focus our attention on how the deformation parameter ϵ of the non-Kerr black hole affects the negative energy state and the efficiency of the energy extraction.

A. The negative energy state of the Penrose process

Let us now consider the trajectory of a test particle with the mass μ on the equatorial plane. With the help of the timelike Killing vector $\xi^a = \left(\frac{\partial}{\partial t}\right)^a$ and spacelike one $\psi^a = \left(\frac{\partial}{\partial \phi}\right)^a$, we have the following conserved quantities along a timelike geodesics on the equatorial plane

$$E = -g_{ab}\xi^a u^b = \left(1 + \frac{\epsilon M^3}{r^3}\right)\left(1 - \frac{2M}{r}\right)u^t + \left(1 + \frac{\epsilon M^3}{r^3}\right)\frac{2aM}{r}u^\phi, \quad (3.1)$$

$$L = g_{ab}\psi^a u^b = -\left(1 + \frac{\epsilon M^3}{r^3}\right)\frac{2aM}{r}u^t + \left(r^2 + a^2 + \frac{a^2 M^3(a^2 + r^2)\epsilon}{r^5} + \frac{2a^2 M}{r}\right)u^\phi, \quad (3.2)$$

where u^b is the four-velocity defined by $u^b = \frac{dx^b}{d\tau}$, τ is the proper time for the spacetime. In Eq. (3.1) or (3.2), the first equality is the basic definition of the energy or angular momentum [10], and the second equality describes the energy or angular momentum of the non-Kerr black hole. Moreover, we can introduce a new conserved parameter

$$\kappa = g_{ab}u^a u^b, \quad (3.3)$$

whose values are given by $\kappa = -1, 0, 1$ corresponding to the timelike, null and spacelike geodesics, respectively.

From Eqs. (3.1), (3.2) and (3.3) we can easily obtain the equation of motion

$$\alpha E^2 - 2\beta E + \gamma = 0, \quad (3.4)$$

with

$$\alpha = \left(r^2 + a^2 + \frac{a^2 M^3(a^2 + r^2)\epsilon}{r^5} + \frac{2a^2 M}{r}\right)\Gamma^{-1}, \quad (3.5)$$

$$\beta = L\left(1 + \frac{\epsilon M^3}{r^3}\right)\frac{2aM}{r}\Gamma^{-1}, \quad (3.6)$$

$$\gamma = -L^2\left(1 + \frac{\epsilon M^3}{r^3}\right)\left(1 - \frac{2M}{r}\right)\Gamma^{-1} - \frac{r^2(r^3 + \epsilon M^3)}{r^3\Delta + a^2\epsilon M^3}(u^r)^2 - \mu^2, \quad (3.7)$$

where

$$\Gamma = (1 + \frac{\epsilon M^3}{r^3})(\Delta + a^2 \frac{\epsilon M^3}{r^3}). \quad (3.8)$$

From Eq. (3.4), we can obtain the energy E

$$E = \frac{\beta + \sqrt{\beta^2 - \alpha\gamma}}{\alpha}, \quad (3.9)$$

where we only choose $+\sqrt{\beta^2 - \alpha\gamma}$ to ensure that the 4-momentum of the particle is future directed. In the Penrose process, the orbit of the particle with negative energy in the ergosphere is the key to extract energy from the non-Kerr black hole. When a particle enters the ergosphere, the timelike Killing vector becomes spacelike one, thus the energy of the particle $E = -g_{ab}\xi^a u^b$ becomes negative. The orbit of the particle with the negative energy E must satisfy the conditions: $\alpha > 0$, $\beta < 0$ and $\gamma > 0$, which can be achieved only if $La < 0$. In Fig. 3, we describe the negative energy state E for the different deformation

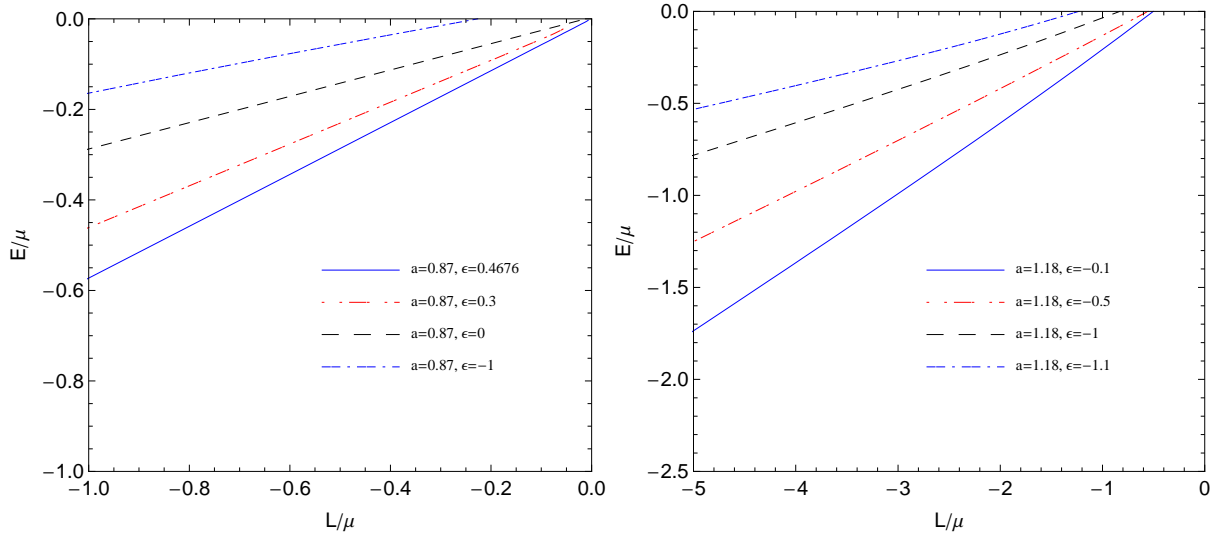


FIG. 3: The negative energy state E allowed for the angular momentum L and rest mass μ of the particles for the different deformation parameter ϵ at a given location near the event horizon inside the ergosphere.

parameter ϵ at a given location near the event horizon inside the ergosphere. We find that the negative energy E increases as the deformation parameter ϵ increases for both the cases

$a > M$ and $a < M$.

According to the Penrose process, the mass of the black hole will change a quantity $\delta M = E$ as a negative particle is injected into the central black hole. Clearly δM can be made as large as we wished by increasing the mass μ of the injected particle. However, there is a lower limit on δM which could be added to the black hole corresponding to $\mu = 0$ and $u^r = 0$ [18]. Evaluating all of the required quantities at the horizon r_H , we can get the lower limit

$$E_{\min} = \frac{L(1 + \frac{\epsilon M^3}{r_H^3}) \frac{2aM}{r_H}}{r_H^2 + a^2 + \frac{a^2 M^3 (a^2 + r_H^2) \epsilon}{r_H^5} + \frac{2a^2 M}{r_H}}. \quad (3.10)$$

From the Eq. (3.10) we can conclude that, in order to extract energy from the black hole, the angular momentum of the injected particle must satisfy $L < 0$, and the deformation parameter ϵ influences the value of E_{\min} .

B. Efficiency of the energy extraction process

The efficiency of the energy extraction process is one of the most important questions in the energetics of the black hole. Thus, it is interesting to study how the deformation parameter ϵ affects the efficiency of the Penrose process [2, 17, 19] for the non-Kerr black hole. To calculate the maximum efficiency of the energy extraction, we take the radial velocity to be zero. Let U_i denotes the four-velocity of the i th particle of the locally nonrotating frame observer [3] at a given radius r , which can be expressed as

$$U_i = u^t(1, 0, 0, \Omega_i), \quad (3.11)$$

with

$$\begin{aligned} u^t &= -\frac{E}{X_i}, & X_i &= -(g_{tt} + g_{t\phi}\Omega_i), \\ \Omega_i &= \frac{-g_{t\phi}(1 + g_{tt}) + \sqrt{(1 + g_{tt})(g_{t\phi}^2 - g_{tt}g_{\phi\phi})}}{g_{\phi\phi} + g_{t\phi}^2}, \end{aligned} \quad (3.12)$$

where Ω_i is the angular velocity of the particle i with respect to an asymptotic infinity observer. In the ergosphere, Ω_i takes the value in the range of $\Omega_- < \Omega < \Omega_+$, where

$$\Omega_{\pm} = \frac{-g_{t\phi} \pm \sqrt{g_{t\phi}^2 - g_{tt}g_{\phi\phi}}}{g_{\phi\phi}}. \quad (3.13)$$

In the Penrose process, an incident particle 1 with the rest mass $\mu_1 = 1$, i.e. $E_1 = 1$, splits into the particle 2 absorbed by the black hole and the particle 3 escaping to infinity. According to the conservational laws of the energy and angular momentum, we get

$$U_1 = \mu_2 U_2 + \mu_3 U_3. \quad (3.14)$$

The efficiency of the Penrose process is defined as

$$\eta = \frac{\mu_3 E_3 - E_1}{E_1} = \mu_3 E_3 - 1. \quad (3.15)$$

The maximum efficiency η can be obtained by the choice of $\mu_2 U_2$ and $\mu_3 U_3$ [19]

$$\mu_2 U_2 = k_2(1, 0, 0, \Omega_-) \quad (3.16)$$

$$\mu_3 U_3 = k_3(1, 0, 0, \Omega_+),$$

where k_2 and k_3 are constants to be determined. With the help of the Eqs. (3.11), (3.12), (3.14) and (3.16), we find

$$\eta = \frac{(\Omega_1 - \Omega_-)(g_{tt} + g_{t\phi}\Omega_+)}{(\Omega_+ - \Omega_-)(g_{tt} + g_{t\phi}\Omega_1)} - 1. \quad (3.17)$$

When the incident particle 1 splits at the horizon r_H , we thus obtain the maximum efficiency

$$\eta_{max} = \left. \frac{\sqrt{1 + g_{tt}} - 1}{2} \right|_{r=r_H}. \quad (3.18)$$

Now, we would like to analyze the effects of ϵ on the efficiency of the rapidly rotating

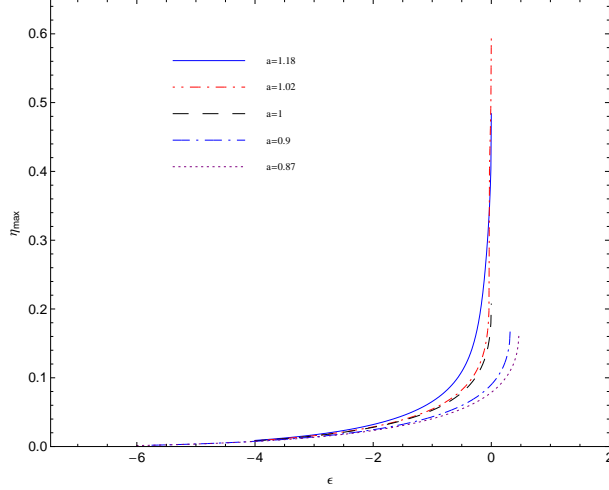


FIG. 4: The Variation of the maximum efficiency of the energy extraction process with the deformation parameter ϵ of rotating non-Kerr black hole. Here we take $M = 1$.

non-Kerr black hole. We calculate the maximum efficiency with the numerical method and present the variation of the maximum efficiency in the energy extraction process with the deformation parameter ϵ , which takes the value in the range (2.9) to guarantee that the non-Kerr black hole has the connected event horizon for a fixed a in Fig. 4. We also present the effects of the parameter ϵ on the maximum efficiency in Table. I and II.

TABLE I: The maximum efficiency η_{\max} of energy extraction process in the non-Kerr black hole depends on the parameter ϵ for $a \leq M$. Here we set $M=1$.

	$a=0.2$	$a=0.4$	$a=0.6$	$a=0.8$	$a=0.9$	$a=0.99$	$a=1$
$\epsilon=0$	0.25%	1.0%	2.7%	5.9%	9.01%	16.2%	20.7%
$\epsilon=0.01$	0.255%	1.082%	2.710%	5.940%	9.1%	17.1%	
$\epsilon=0.02$	0.256%	1.083%	2.73%	5.975%	9.200%	19.025%	
$\epsilon=0.2$	0.268%	1.142%	2.915%	6.71%	11.58%		
$\epsilon=0.3$	0.275%	1.175%	3.026%	7.187%	14.594%		
$\epsilon=0.4$	0.282%	1.209%	3.242%	8.442%			

Obviously, it is shown that the maximum efficiency of the Penrose process can be enhanced as the parameter ϵ increases. It is interesting to note that, for $a > M$, the non-Kerr metric describes a superspinning black hole [5, 23], the maximum efficiency can exceed 60%, while it is only 20.7% for the extremal Kerr black hole. This result is reasonable, because in the Sec. II, we investigate the ergosphere and find that the maximum thickness of the

TABLE II: The maximum efficiency η_{\max} of energy extraction process in the non-Kerr black hole depends on the parameter ϵ for $a > M$. Here we set $M=1$.

	$a=1.001$	$a=1.01$	$a=1.1$	$a=1.15$	$a=1.2$
$\epsilon=-0.00001$	60.739%	59.954%	52.885%	49.487%	46.406%
$\epsilon=-0.0001$	59.577%	58.806%	51.859%	48.520%	45.492%
$\epsilon=-0.001$	56.922%	56.186%	49.547%	46.353%	43.455%
$\epsilon=-0.01$	50.088%	49.492%	43.945%	41.201%	38.683%
$\epsilon=-0.1$	13.136%	13.844%	24.878%	26.231%	25.901%
$\epsilon=-1$	5.278%	5.360%	6.087%	6.420%	6.638%

ergosphere on the equatorial plane increases as the deformation parameter ϵ increases. Especially, for $a = 1.18$ and $\epsilon = -0.1$, the thickness of the ergosphere on the equatorial plane is much thicker than that of the extremal Kerr black hole ($a = 1$, $\epsilon = 0$) in Fig. 2. If the values of a and ϵ change gradually, by accretion or any other process, from $a < M$ to $a > M$ and from $\epsilon > 0$ to $\epsilon < 0$ we should expect a continuous change of the energy extraction intuitively. Why is it not so? From the Eq. (3.18), we find that the maximum efficiency ($\eta_{\max} = \frac{\sqrt{1+g_{tt}}-1}{2}\big|_{r=r_H}$) is related to the event horizon r_H of the non-Kerr black hole. In Fig. 5, by taking $\epsilon = -0.001$ and considering the values of a changes gradually from $a = 1$ to 1.001, we find the variation of the event horizon r_H is not continuous. Therefore, we can not obtain a continuous change of the energy extraction for the process by taking a from $a < M$ to $a > M$ (or from $\epsilon > 0$ to $\epsilon < 0$).

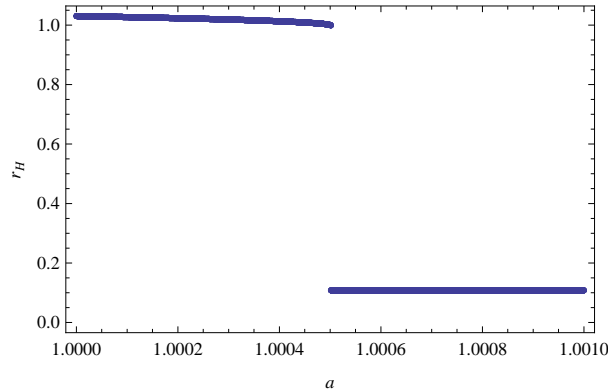


FIG. 5: The variation of the event horizon with the rotating parameter a of a rotating non-Kerr black hole with $M = 1$ and $\epsilon = -0.001$.

IV. SUMMARY

In this paper, we present a detail analysis of the properties of the ergosphere in the rotating non-Kerr black hole proposed recently by Johannsen and Psaltis [5] to test gravity in the regime of the strong field in the future astronomical observations. We now summarize our results as follows: (1) We present the restricted conditions on the deformation parameter ϵ to guarantee that the non-Kerr black hole has the connected horizons (see Eq. 2.9 and Fig. 1). (2) We show that the ergosphere is sensitive to the deformation parameter ϵ (see Fig. 2) and the shape of the ergosphere becomes thick with increase of the deformation parameter ϵ . (3) We find that, comparing with the Kerr black hole, the deformation parameter ϵ not only enlarges the negative energy E (see Fig. 3) but also enhances the maximum efficiency of the energy extraction process (see tables I-II and Fig. 4). Moreover, the maximum efficiency can exceed 60% for the non-Kerr compact objects with $a > M$. The influence of the deformation parameter ϵ on the maximum efficiency presents a good theoretical opportunity to distinguish the non-Kerr black hole from the Kerr one and to test whether or not the current black-hole candidates are the black holes predicted by Einstein's general relativity. However, we think such a test is not possible at present.

V. ACKNOWLEDGMENTS

This work was supported by the National Natural Science Foundation of China under Grant No. 11175065, 10935013; the National Basic Research of China under Grant No. 2010CB833004; the SRFDP under Grant No. 20114306110003; PCSIRT, No. IRT0964; the Hunan Provincial Natural Science Foundation of China under Grant No 11JJ7001; Hunan Provincial Innovation Foundation For Postgraduate under Grant No CX2011B185; and Construct Program of the National Key Discipline.

-
- [1] W. Israel, Phys. Rev. **164** (1967) 1776; W. Israel, Commun. Math. Phys. **8** (1968) 245; B. Carter, Phys. Rev. Lett. **26** (1971) 331; S. W. Hawking, Commun. Math. Phys. **25** (1972) 152; D. C. Robinson, Phys. Rev. Lett. **34** (1975) 905.

- [2] R. Penrose, Riv. Nuovo Cim. Numero Speciale **1** (1969) 252.
- [3] C. M. Will, Living Rev. Rel. **9** (2005) 3.
- [4] F. Caravelli and L. Modesto, Class. Quant. Grav. **27** (2010) 24502.
- [5] T. Johannsen and D. Psaltis, Phys. Rev. D **83** (2011) 124015.
- [6] C. Bambi and L. Modesto, arXiv:1107.4337 [gr-qc].
- [7] S. A. Hughes, arXiv:1002.2591; D. Psaltis and T. Johannsen, J. Phys. Conf. Ser. **283**, (2011) 2030; T. Johannsen and D. Psaltis, Astrophys. J. **716**, (2010) 187 ; T. Johannsen and D. Psaltis, Astrophys. J. **718**, (2010) 446 ; T. Johannsen and D. Psaltis, Astrophys. J. **726**, (2011) 11 .
- [8] F. D. Ryan, Phys. Rev. D **52**, (1995) 5707; F. D. Ryan, Phys. Rev. D **56**, (1997)1845 ; F. D. Ryan, Phys. Rev. D **56**, (1997) 7732 ; L. Barack and C. Cutler, Phys. Rev. D **69**, (2004) 082005 ; J. Brink, Phys. Rev. D **78**, (2008)102001 ; C. Li and G. Lovelace, Phys. Rev. D **77**, (2008) 064022 ; T. A. Apostolatos, G. Lukes-Gerakopoulos, and G. Contopoulos, Phys. Rev. Lett. **103**, (2009)111101 .
- [9] C. Bambi and L. Modesto, arXiv:1110.2768 [gr-qc].
- [10] C. Bambi, arXiv:1110.0687[gr-qc].
- [11] P. Pani, C. F. B. Macedo, L. C. B. Crispino and V. Cardoso, arXiv:1109.3996 [gr-qc].
- [12] T. Johannsen, arXiv:1105.5645v1 [astro-ph.HE].
- [13] S. Chen and J. Jing, arXiv:1110.3462 [gr-qc].
- [14] M. Kozfowski and M. Abramowicz, Astr. Astrophys. **63**, (1978) 209.
- [15] N. I. Shakura and R. A. Sunyaev, Astr. Astrophys. **24**, (1973) 337.
- [16] R. D. Blandford and R. L. Znajek, Mon. Not. R. astr. Soc **179**, (1977) 433.
- [17] S. Chandrasekhar, *The Mathematical Theory of black holes* (Oxford University Press, New York, 1983)
- [18] C. W. Misner, K.S. Thorne, and J.A. Wheeler, *Gravitation* (SanFrancisco, Freeman, 1973)
- [19] M. Bhat, S. Dhurandhar and N. Dadhich, Astrophys. J. **6**, (1985) 85;
S. Parthasarathy, S. M. Wagh, S. V. Dhurandhar and N. Dadhich, Astrophys. J., **307**, (1986) 38
- [20] K. Prabhu and N. Dadhich, Phys.Rev.D. **81**, (2010) 024011
- [21] M. Nozawa and K. Maeda, Phys. Rev. D **71** (2005) 084028.
- [22] A. Abdujabbarov and B. Ahmedov, Phys. Rev. D **84** (2011) 044044.
- [23] C. Bambi and K. Freese, Phys.Rev.D. **79**, (2009) 043002.